

Modeling and control of flexible loads for frequency regulation services considering compensation of communication latency and detection error



Hongxun Hui^a, Yi Ding^{a,*}, Yonghua Song^{b,a}, Saifur Rahman^c

^a College of Electrical Engineering, Zhejiang University, Hangzhou, China

^b Department of Electrical and Computer Engineering, University of Macau, Macau, China

^c Advance Research Institute, Virginia Tech, United States

HIGHLIGHTS

- The flexible loads are developed as the ON-OFF and continuously adjustable loads.
- The communication latency is considered in the centralized control model.
- The frequency detection error is considered in the distributed control model.
- The frequency detection error can be reduced by the proposed hybrid control method.
- The estimation accurate of the frequency can be improved by the modification model.

ARTICLE INFO

Keywords:

Demand response
Frequency regulation service
Flexible loads
Communication latency
Frequency detection error

ABSTRACT

Demand response has been widely utilized to provide frequency regulation service for the power systems by adjusting the power consumption of flexible loads. The frequency regulation service is time-sensitive and generally realized by direct load control, due to the quick response requirement (generally a few seconds). Most of the existing studies assume that the control on flexible loads can be implemented immediately without communication latency (CML), and the system frequency deviations can be detected without errors (FDE). However, in reality, the CML and FDE are ever-present during the control process and can influence the effectiveness of regulation significantly. To address this issue, this paper develops the aggregation models of ON-OFF flexible loads and continuously adjustable flexible loads, respectively. The centralized and distributed control methods considering the CML and FDE are developed, respectively. On this basis, a novel hybrid control method is proposed to compensate the CML and FDE, in which the modification method is developed for improving the estimation accuracy of the FDE. The results in the numerical studies show that the maximum system frequency deviation extends from -0.112 Hz to -0.120 Hz and -0.221 Hz due to the FDE and CML, respectively. After the modification by the proposed hybrid control method, the maximum frequency deviation is decreased to -0.110 Hz, which is almost equal to the ideal value when there is no FDE and CML. Therefore, this research can compensate the CML and FDE well, which is useful for guiding demand response projects in smart grid.

1. Introduction

The large-scale blackouts in power systems are increasing in recent years, which have caused tremendous negative influences on people's life. For example, the blackout in Brazil resulted in 22.5% grid output on March 21, 2018 [1], and the blackout in Taiwan on August 15, 2017 affected 6.68 million households [2]. These blackouts raise awareness of the importance of the frequency regulation service (FRS) for maintaining the system balance between power supply and demand.

Traditionally, the FRS is provided by the generation units [3], such as the thermal power generators and the gas turbine units [4]. However, traditional generation units may be phased out in the near future, which will lead to insufficient reserve capacities for FRS, especially with the increasing fluctuations brought by the high penetration of renewable energies [5].

The progressed information and communication technologies make the customers' loads smarter, which offers an alternative way to provide FRS from demand side by adjusting the power consumption of flexible

* Corresponding author.

E-mail address: yiding@zju.edu.cn (Y. Ding).

<https://doi.org/10.1016/j.apenergy.2019.04.191>

Received 15 January 2019; Received in revised form 27 March 2019; Accepted 29 April 2019

0306-2619/© 2019 Published by Elsevier Ltd.

Nomenclature

Acronyms

AC	air conditioner
CCM	centralized control method
CFL	continuously adjustable flexible load
CML	communication latency
DCM	distributed control method
DLC	direct load control
DR	demand response
FDE	frequency detection error
FL	flexible load
FRS	frequency regulation service
HCM	hybrid control method
IAC	inverter air conditioner
MFD	maximum frequency deviation
MVUE	minimum-variance unbiased estimator
OFL	ON-OFF flexible load
PMU	phasor measurement unit
RT	recovery time

Variables and parameters

i	the i -th OFL (subscript)
j	the j -th CFL (subscript)
k	the k -th historical data (subscript)
r	the rated value (subscript)
N	total number of OFLs
N_{OFF}	total number of OFLs that are switched from ON-state to OFF-state
M	total number of CFLs
K	total number of historical data
Φ	the set of OFLs
Ψ	the set of CFLs
$P_{OFL,r,i}$	the rated power of the i -th OFL
$P_{OFL,r,avg}$	the average rated power of the aggregated OFLs
$P_{OFL,total}$	the total power of OFLs
$P_{CFL,j}$	the operating power of the j -th CFL
ΔP_D	the disturbance load
$S_{OFL,i}$	the operating state of the i -th OFL
$\kappa_{CFL,j}$	the slope coefficient of the j -th CFL
$l_{CFL,j}$	the intercept coefficient of the j -th CFL
$\Delta_{OFL,i}^{THR}$	the frequency deviation threshold of the i -th OFL to

	provide FRS
$f_{CFL,j}$	the operating frequency of the j -th CFL
$f_{CFL,j}^{ADI}$	the operating frequency of the j -th CFL after the FRS
$f_{CFL,j}^{\min}$	the lower limit of the frequency regulation of the j -th CFL
$f_{CFL,j}^{\max}$	the upper limit of the frequency regulation of the j -th CFL
f_{PMU}	the measured system frequency deviation by the PMU
f_r	the rated frequency of the power system
Δf_s	the system frequency deviation
Δf_s^{\min}	the minimum threshold for participating in FRS
Δf_s^{\max}	the maximum threshold for participating in FRS
$\Delta f_{TC,i}$	the system frequency deviation measured by the i -th terminal controller
$\widehat{\Delta f}_{TC,i}$	the modified value of the system frequency deviation by the i -th terminal controller
$\Delta f_{e,i}$	the system frequency detection error of the i -th terminal controller
t_{cml}	the total communication latency in the CCM
t_{meas}	the communication latency during the measurement process
t_{up}/t_{down}	the communication latency during the uplink/downlink process
t_{cal}	the communication latency during the calculation procedure
t_{ctrl}	the communication latency during the action process
T_g	the time constant of the speed governor
T_t	the time constant of the turbine
T_r	the time constant of the reheat process
F_{HP}	the power fraction of the high-pressure turbine
R	the proportional gain of the generator
K	the integral gain of the generator
H	the generator inertia
K_D	the load-damping factor
X_i	The set of the system frequency detection error of the i -th terminal controller
μ_i	the FDE distribution expectation of the i -th terminal controller
σ_i^2	the FDE variance of the i -th terminal controller
E_i	the MVUE of the FDE distribution expectation of the i -th terminal controller
S_i^2	the MVUE of the FDE variance of the i -th terminal controller
ξ_i	the correction value of the system frequency deviation by the i -th terminal controller

loads (FLs) [6], named as demand response (DR) [7]. The DR projects can generally be divided into two categories: the price-based DR and incentive-based DR [8]. The price-based DR is to influence customers' power consumption through the time-varying electricity prices based on the electricity cost in different periods [9]. The main purpose is to increase the system social welfare or decrease the generation cost. Hence, it is also named market-led or economic-based DR [10]. In contrast, the incentive-based DR is by offering fixed or time-varying payments to motivate the customers to reduce the electricity usage during power system stress periods [9], which is also named system-led, emergency-based or stability-based DR [10]. The main purpose is to ensure the power systems' security and stability operation by controlling FLs directly [11,12]. Therefore, the FRS, which needs a quick response to the system fluctuations (generally 10–30 s for the primary frequency regulation and 30 s to 15 min for the secondary frequency regulation) [3], should be implemented by the incentive-based DR. The most extensive approach of the incentive-based DR is the direct load control (DLC) method [13].

Many studies have been down to verify the effectiveness of the DLC.

For example, a hardware of smart home management system is designed with the communication, sensing technology and machine learning algorithm to realize the direct control of household appliances in [14], while the communication delay is not considered. The air conditioners are regard as one of the most important flexible loads and regulated by the control centre to provide reserve capacities for the power systems in [15,16], while the power system frequency is assumed to be detected instantaneously and the loads can be controlled without time delay. However, the communication delay and control delay cannot be avoided based on the current technologies. The thermostatic loads are controlled for system frequency regulation considering daily demand profile and progressive recovery in [17] and [18], while the system frequency is supposed to be monitored without errors. The deep learning-based techniques and the self-learning coordinated control of FLs are proposed in [19] and [20], respectively, for the load forecasting and the guarantee of customers' comfort, while power consumption data is assumed as ideal values. Besides, it is proved that the customers can get benefits in real time distribution energy market when they participate in DR [21]. Some demonstration

projects of DR have also been carried out. For example, the EcoGrid EU is implemented in Bornholm, Denmark to make small end-customers provide regulation services to assist the system balance with high penetration of renewable energies [22]. The DR project with the name of friendly interactive system of supply and demand in Jiangsu Province, China, is carried out to decrease the load peak-valley difference by controlling customers' household appliances [23].

Most of the existing studies on the control of FLs assume that the control can be implemented immediately without communication latency (CML), and the power system's frequency deviation can be monitored accurately without measurement errors. In fact, the CML and the frequency detection error (FDE) are ever-present in the control process of FLs [24]. Two typical control framework are taken as examples, the centralized control method (CCM) and the distributed control method (DCM). In CCM, the CML can be introduced by sensing equipment and actuators, including the frequency measurement delay, the data uplink delay, the data calculation delay, the control downlink delay and the terminal controller delay [25]. The platform with hardware and software is set up in [26] to test the CML during the DLC process. The results show that the FLs can be switched off between 3.3 s and 4.6 s, instead of instant. In the experimental demonstration of frequency regulation by commercial buildings [27], the CML is considered too large to be neglected, where about 20 s are reserved to account for the CML and the fan transients. The negative effects of CML are simulated and experimented in [28–32], where the CML can decrease the effectiveness of DR for providing FRS and even bring fluctuations to the power systems along with the increase of the delay time. In [24], the CML less than 0.25 s is proved to be “safe” with respect to oscillatory instability, while the CML exceeding 0.5 s can result in system instability on the test. In [33], the FLs are able to regulate the system frequency successfully for the latencies of up to 0.3 s, while the frequency will be unstable when the latency is 0.5 s. In [34], the performance of the FRS is deteriorated when the latency is 0.2 s, and even worse than the scenario without DR if the latency reaches 0.4 s. In a word, the FRS is time-sensitive, whose effectiveness can be impacted significantly by the CML.

Although many existing studies have gotten the conclusions that the CML has negative influence on the DR projects, the compensation method to reduce the CML's impact is rarely studied. Indeed, the most direct method for decreasing the CML is to upgrade the communication equipment, while the cost may be unaffordable and will make the DR projects uneconomic compared with traditional FRS provided by generation units. In [35], the CML's impact on the stability region of the FLs' control parameters is studied, which illustrates that the optional region will be smaller with the increasing of CML. However, how to decrease the CML and increase the control parameters' domain are not further studied. In [36], the fuzzy-PI-based coordinator is proposed to connect the FLs and the traditional generators, so that the generators can receive the input signals from FLs' to change the generating state for mitigating the fluctuations brought by the CML. However, this method increases the regulation burdens of the generators, especially with the increasing capacity of FLs. The *Padé* approximation is used in [34] and [37] to linearize the power system with DR and CML, while it is a linearization method and has no effect on the compensation of CML. In [38], the stochastic predictive controller and *Kalman* filter-based state estimation techniques are proposed to reduce the effects of CML, while this method mainly pays attention to the state estimation and control of FLs. The system frequency measurement delay, the data uplink delay and the calculation delay are not considered.

Apart from the CCM, the DCM is another mainstream approach for implementing DR, in which the terminal controller can monitor the system frequency deviation locally. The CML can be decreased compared with the CCM [39]. However, in the perspective of FDE, the frequency deviation in CCM is generally detected by some precision instruments installed in power systems, e.g., the phasor measurement unit (PMU), so that the FDE in CCM can be neglected [40]. In DCM,

considering the manufacturing cost of the large number of terminal controllers, the accuracy of the frequency detection cannot be the same with that by the PMU [41]. The FDE can lead to the DR capacity control errors and even wrong actions, which may result in a large response bias and threaten the power systems' stability, especially with the increasing scale of FLs.

To address these challenges, this paper proposes a novel hybrid control method (HCM), which combines the advantage of DCM on the short CML, and the advantage of CCM on the small FDE. Firstly, the control parameters are set by the control centre to each terminal controller before the implementation of the FRS. Then, the terminal controllers can monitor the system frequency deviation locally and take action to provide regulation capacities, so that the CML can be decreased significantly. In order to decrease the FDE brought by the terminal controllers, the FDE modification model is proposed to modify the measurement values of the system frequency. The implementation method is that the control centre sends the accurate frequency deviation value detected by the PMU to each terminal controller after each dispatch. Then the FDE modification model is developed based on the statistical data of the measured values by the terminal controllers and PMU, which can be updated with the increase of the historical statistical data.

The originality and contributions of this paper can be summarized as follows:

- (1) The aggregation models of FLs are developed according to two categories, the ON-OFF FLs (OFLs) and the continuously adjustable FLs (CFLs). The previous studies mainly pay attention to the OFLs, while the CFLs are commonly overlooked. The power consumption of CFLs in the power systems is increasing rapidly nowadays (e.g., the inverter air conditioners), and proved to be more suitable for providing FRS [16].
- (2) Based on the aggregation model of OFLs and CFLs, the frameworks, control algorithms and system frequency response models of the CCM and DCM are proposed, respectively. The CML and the FDE are considered in the frameworks and models, which are usually not considered in the previous studies.
- (3) A novel framework and implementation procedure of the HCM are proposed based on the CCM and DCM, which can avoid the CML and reduce the FDE during the control process of FLs. Moreover, the modification model is developed for improving the estimation accuracy of the FDE, in which the simplified iterative approach for updating the modification parameters is also proposed to decrease the data storage space and computation load of the terminal controllers, respectively.
- (4) The effectiveness of the proposed models and methods is illustrated in case studies, in which the three control methods (i.e., the CCM, DCM and HCM) are compared. The results show that, under the same disturbance load, the maximum frequency deviation and the recovery time extend from -0.112 Hz and 75.8 s to -0.221 Hz and 272.9 s, respectively, due to the influence of the CML. The proposed HCM can modify the system frequency detection errors and make the FLs take action more accurately, where the maximum frequency deviation can be reduced from -0.120 Hz to -0.110 Hz. Therefore, this research can compensate the CML and FDE well, which is useful for guiding demand response projects in smart grid.

The remainder of this paper is organized as follows. The models of FLs are developed in Section 2, including the OFLs and CFLs. Section 3 presents the frameworks, the control algorithms, and the system frequency response models of the CCM and DCM, respectively. Section 4 presents the framework, the FDE modification model, and the implementation procedure of the proposed HCM. Numerical studies are illustrated in Section 5. Finally, Section 6 concludes this paper.

2. Modelling of flexible loads for frequency regulation service

As the literature review in Section 1, DLC is the most extensive and effective method to regulate FLs for providing FRS [10]. Generally, the DCL is implemented by switching the operating state of FLs between ON- and OFF-state [11,12]. This kind of FLs are named ON-OFF flexible loads (OFLs). The other kind of FLs, which have converters and inverters (e.g., inverter air conditioners), can be controlled by adjusting the motors' or compressors' operating frequency continuously to regulate the power consumption [16]. Considering the rapidly expanding number of inverter air conditioners in the power consumption [42], this kind of FLs are considered separately from the OFLs in this paper and named continuously adjustable flexible loads (CFLs). Both the OFLs and CFLs are modelled in this section.

2.1. ON-OFF flexible loads

The set of OFLs are denoted as $\Phi = \{i | 1 \leq i \leq N, i \in \mathbf{Z}\}$, where N is the total number of OFLs. The power consumption of OFLs can be calculated by the rated power $P_{OFL,r,i}$ and the corresponding operating state $S_{OFL,i}(t)$, which can be expressed as

$$P_{OFL,total}(t) = \mathbf{P}_{OFL,r}^T \mathbf{S}_{OFL} = \sum_{i=1}^N P_{OFL,r,i} S_{OFL,i}(t) \quad (1)$$

where $\mathbf{P}_{OFL,r}$ and \mathbf{S}_{OFL} are the set of OFLs' rated powers and operating states, and can be expressed as $\mathbf{P}_{OFL,r} = [P_{OFL,r,1}, P_{OFL,r,2}, \dots, P_{OFL,r,N}]^T$ and $\mathbf{S}_{OFL} = [S_{OFL,1}(t), S_{OFL,2}(t), \dots, S_{OFL,N}(t)]^T$, respectively. The operating state has two values, i.e., $S_{OFL,i}(t) \in \{0, 1\}$, where 0 is the OFF-state and 1 is the ON-state.

As for the large-scale FLs, the total power of OFLs can also be estimated by the average power from the historical statistical data, which can be expressed as

$$P_{OFL,total}(t) = P_{OFL,r,avg} \sum_{i=1}^N S_{OFL,i}(t) \quad (2)$$

where $P_{OFL,r,avg}$ is the OFLs' average rated power. In this way, the total regulation power of OFLs for providing FRS can be simplified to adjust

the number of OFLs operating in the ON-state.

2.2. Continuously adjustable flexible loads

The CFLs' power consumption is mainly related to the operating frequency of the motors (the compressors in the inverter air conditioners belong to a kind of motors) [16], and can be expressed as

$$P_{CFL,j}(t) = \kappa_{CFL,j} f_{CFL,j}^2(t) + l_{CFL,j} \quad (3)$$

where $P_{CFL,j}$ and $f_{CFL,j}$ are the operating power and corresponding operating frequency of the CFL- j , respectively. The $\kappa_{CFL,j}$ is the proportionality coefficient that reflects the power consumption related to the operating frequency of the compressor. The $l_{CFL,j}$ is the constant coefficient of the power consumption, which is not related to the compressor's operating frequency, such as the power consumption by the inverter air conditioner's control panel and the indicator light. Denoting the set of CFLs is $\Psi = \{j | 1 \leq j \leq M, j \in \mathbf{Z}\}$, where M is the total number of CFLs. The CFLs' coefficients are expressed as $\mathbf{K}_{CFL} = [\kappa_{CFL,1}, \kappa_{CFL,2}, \dots, \kappa_{CFL,M}]^T$ and $\mathbf{L}_{CFL} = [l_{CFL,1}, l_{CFL,2}, \dots, l_{CFL,M}]^T$. The set of operating frequencies are $\mathbf{F}_{CFL} = [f_{CFL,1}(t), f_{CFL,2}(t), \dots, f_{CFL,M}(t)]^T$. Then, the total power of CFLs can be calculated as

$$P_{CFL,total}(t) = \mathbf{K}_{CFL}^T \mathbf{F}_{CFL} + \mathbf{L}_{CFL}^T \mathbf{1}_M \quad (4)$$

where the frequency regulation ranges of CFLs can be expressed as $f_{CFL,j}(t) \in [f_{CFL,j}^{\min}, f_{CFL,j}^{\max}]$.

3. Control framework of flexible loads considering the communication latency and frequency detection error

Based on the two typical FLs (OFLs and CFLs), the control frameworks are developed in this section, including the centralized control method (CCM) and the distributed control method (DCM). Moreover, considering the pros and cons of the two kinds of methods, the communication latency (CML) model is supplemented in the CCM, and the frequency detection error (FDE) is considered in the DCM.

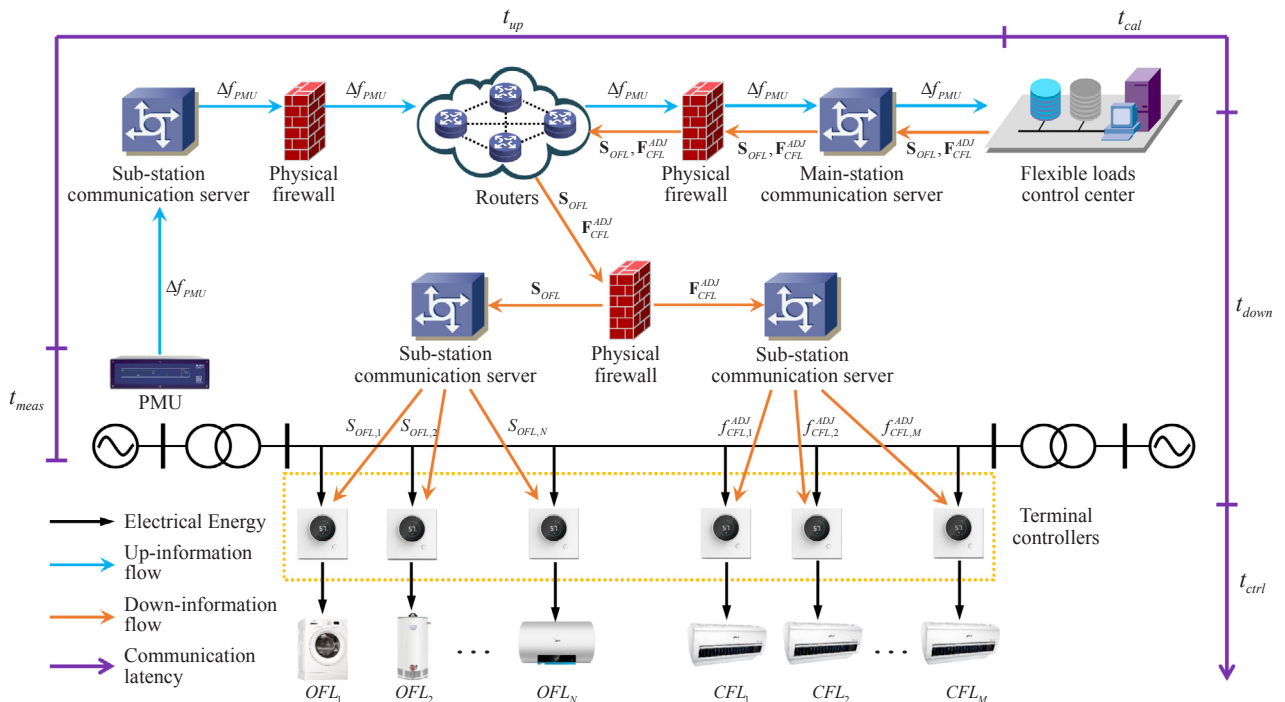


Fig. 1. The framework of the centralized control method.

3.1. Centralized control method

(1) Framework of the centralized control method

Fig. 1 shows the framework of the CCM. The phasor measurement unit (PMU) installed on the bus acts as the frequency deviation sensor, which can monitor the system frequency f_{PMU} and get the deviation value Δf_{PMU} , as shown in Eq. (5).

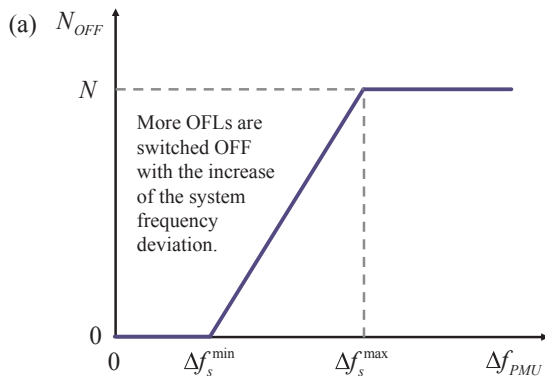
$$\Delta f_{PMU}(t) = f_r - f_{PMU}(t) \quad (5)$$

However, due to the synchronized sampling, data packaging and sending process, the PMU results in millisecond delay (t_{meas}) [25]. Then, the frequency deviation data is transmitted to the control centre. In the uplink transmission process, the data has to pass through the sub-station communication server, the physical firewall, the routers and the main-station communication server, which causes the uplink delay (t_{up}). Next, based on these FLs' operating states (S_{OFL} , F_{CFL}) and the frequency deviation value (Δf_{PMU}), the control centre calculates the control instructions of the OFLs and CFLs. The delay of the calculation procedure is expressed as t_{cal} . After that the control centre sends the regulation signals to the terminal controllers by the downlink transmission process, which leads to the downlink delay (t_{down}). Finally, the terminal controllers take action to adjust the operating state of the FLs, including the ON-OFF control of OFLs and frequency regulation control of CFLs, where the delay is expressed as t_{ctrl} . Therefore, the total CML of the CCM can be expressed as

$$t_{cml} = t_{meas} + t_{up} + t_{cal} + t_{down} + t_{ctrl} \quad (6)$$

(2) Algorithm in the control centre

The control centre has two algorithms for the OFLs and CFLs, respectively. The algorithm for the OFLs is to calculate the total number of OFLs, which should be switched OFF from the ON-state. The control method is illustrated in Fig. 2(a), where the minimum and maximum frequency deviation thresholds of the power system are expressed as Δf_s^{\min} and Δf_s^{\max} , respectively. When the system frequency deviation is less than the minimum threshold Δf_s^{\min} , the OFLs will not be controlled to provide the regulation service. It can be regard as the dead band of the controllers to avoid the frequent adjustment of OFLs when facing small system frequency fluctuations. When the system frequency is larger than the maximum threshold Δf_s^{\max} , all the OFLs will be switched to OFF-state to provide the regulation service. In this condition, the controlled number of OFLs reaches the maximum value and cannot increase. If the system frequency deviation is between the Δf_s^{\min} and Δf_s^{\max} , more OFLs will be controlled with the increase of Δf_{PMU} , where the proportional value of the controlled number of OFLs in the total available number of OFLs can be expressed as $(\Delta f_{PMU}(t) - \Delta f_s^{\min}) / (\Delta f_s^{\max} - \Delta f_s^{\min})$. Therefore, the control algorithm of OFLs can be described as



$$N_{OFF}(\Delta f_{PMU}(t)) = \begin{cases} 0, & \Delta f_{PMU}(t) \leq \Delta f_s^{\min} \\ \frac{\Delta f_{PMU}(t) - \Delta f_s^{\min}}{\Delta f_s^{\max} - \Delta f_s^{\min}} N, & \Delta f_s^{\min} \leq \Delta f_{PMU}(t) \leq \Delta f_s^{\max} \\ N, & \Delta f_{PMU}(t) \geq \Delta f_s^{\max} \end{cases} \quad (7)$$

In order to decrease the impact of DR on customers' comfort, the total regulation times of each OFL are recorded as $R_{OFL} = [r_{OFL,1}, r_{OFL,2}, \dots, r_{OFL,N}]^T$, which are arranged in the order from small to large. The first number of OFLs (N_{OFF}) will be selected and switched OFF. In this manner, the controlled times of the OFLs can be approximately equal to avoid the frequent schedule of one specific OFL.

The control algorithm of the CFLs is for calculating the adjusting values of the operating frequencies to change the corresponding operating power. The control method is illustrated in Fig. 2(b), where the minimum and maximum frequency deviation thresholds of the power system are the same with that in Fig. 2(a). When the system frequency deviation is less than the minimum threshold Δf_s^{\min} , the CFLs will remain the original operating states and not be controlled to provide the regulation service. It can be regard as the dead band of the controllers to avoid the frequent adjustment of CFLs when facing small system frequency fluctuations. When the system frequency is larger than the maximum threshold Δf_s^{\max} , all the CFLs' compressors will be adjusted to the minimum operating frequencies to participate in regulation service. At this time, the regulation capacity provided by CFLs reaches the maximum value. If the system frequency deviation is between the Δf_s^{\min} and Δf_s^{\max} , the CFLs' operating frequencies will be adjusted to smaller values with the increase of Δf_{PMU} . As shown in Fig. 2(b), the proportional value of the adjustment of CFLs' operating frequencies can be expressed as $(\Delta f_{PMU}(t) - \Delta f_s^{\min}) / (\Delta f_s^{\max} - \Delta f_s^{\min})$. Therefore, the operating frequency of the CFL-j after the regulation can be expressed as

$$f_{CFL,j}^{ADJ}(\Delta f_{PMU}(t)) = \begin{cases} f_{CFL,j}(t), & \Delta f_{PMU}(t) \leq \Delta f_s^{\min} \\ f_{CFL,j}(t) - \frac{\Delta f_{PMU}(t) - \Delta f_s^{\min}}{\Delta f_s^{\max} - \Delta f_s^{\min}} (f_{CFL,j}(t) - f_{CFL,j}^{\min}), & \Delta f_s^{\min} \leq \Delta f_{PMU}(t) \leq \Delta f_s^{\max} \\ f_{CFL,j}^{\min}, & \Delta f_{PMU}(t) \geq \Delta f_s^{\max} \end{cases} \quad (8)$$

The set of the operating frequencies can be expressed as $F_{CFL}^{ADJ} = [f_{CFL,1}^{ADJ}(t), f_{CFL,2}^{ADJ}(t), \dots, f_{CFL,M}^{ADJ}(t)]^T$. With the recovery of the power system frequency, the CFLs' operating frequencies will also restore to the original values, so that the FRS has little or no effect on the customers' comfort in the short period of regulation process (generally 10–30 s for primary frequency regulation and 30 s–15 min for secondary frequency regulation) [3].

(3) System frequency response model of the centralized control method

Based on the control algorithms and the CML model of CCM, the

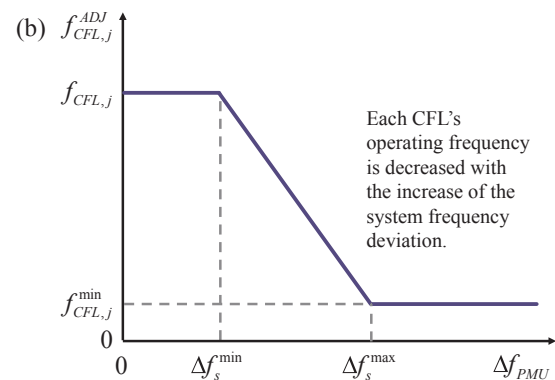


Fig. 2. The control algorithms of the centralized control method: (a) the OFLs, (b) the CFLs.

system frequency response model can be developed, as shown in Fig. 3. In this system model, the reheat steam generator is taken as an example of generation units, which includes the speed governor, the reheat steam turbine and the generator [16,41,45]. When the disturbance load ΔP_D is added to the system suddenly, the system deviation Δf_s will occur and be detected by the PMU. The FLs will decrease the power consumption and the reheat steam generator will increase the power generation to enable the system frequency to recover to the rated value.

It can be seen from the Fig. 3 that the power generation deviation ΔP_G can be derived from the reheat steam turbine model and the speed governor model. The speed governor model is influenced by the proportional gain (R) and the integral gain (K). Therefore, the ΔP_G can be derived as [16]

$$\begin{aligned} \Delta P_G &= \frac{F_{HP}T_r s + 1}{(T_r s + 1)(T_g s + 1)} \cdot \frac{1}{T_g s + 1} \left(-\frac{K}{s} - \frac{1}{R} \right) \Delta f_s \\ &= -\frac{(1/R + K/s)(F_{HP}T_r s + 1)}{(T_g s + 1)(T_r s + 1)} \Delta f_s \end{aligned} \quad (9)$$

where T_g , T_t and T_r are the time constants of the speed governor, the turbine and the reheat process, respectively. F_{HP} is the high pressure turbine's power fraction. R and K are the proportional and integral gains, respectively. Moreover, H and K_D are the generator inertia and the load-damping factor, respectively. Based on Eqs. (1)–(8), the regulation power of the OFLs and the CFLs in the CCM can be expressed as

$$\Delta P_{OFL,total} = -P_{OFL,r,avg} N_{OFF} (\Delta f_{PMU}) \cdot e^{-st_{ctrl}} \quad (10)$$

$$\Delta P_{CFL,total} = K_{CFL}^T (F_{CFL}^{ADJ} - F_{CFL}) \cdot e^{-st_{ctrl}} \quad (11)$$

3.2. Distributed control method

(1) Framework of the distributed control method

Fig. 4 shows the framework of the DCM, where the terminal controllers can monitor the system frequency deviation ($\Delta f_{TC,i}$) locally. However, different from the measurement accuracy of the PMU in the CCM, the system frequency detection error (FDE) by the terminal controllers cannot be neglected, which can be expressed as

$$\Delta f_{e,i}(t) = \Delta f_s(t) - \Delta f_{TC,i}(t) \quad (12)$$

where Δf_s , $\Delta f_{TC,i}$ and $\Delta f_{e,i}$ are the actual frequency deviation, the measured frequency deviation and the FDE, respectively. Moreover, the control centre presets the frequency deviation thresholds to each terminal controller before the FRS occurrence, so that the terminal controllers can take action when the system frequency deviation reaches the threshold values. In this manner, the control centre and the terminal controllers do not need to keep communication in real-time,

and the CML can be decreased significantly.

(2) Algorithm in the terminal controllers

As for OFLs, the terminal controllers are set frequency deviation thresholds ($\Delta f_{OFL,i}^{THR}$). If the measured frequency deviation ($\Delta f_{TC,i}$) exceeds the threshold value, the corresponding OFLs will be switched OFF. The threshold values obey uniform distribution between Δf_s^{\min} and Δf_s^{\max} , which can be expressed as

$$\Delta f_{OFL,i}^{THR} \sim U(\Delta f_s^{\min}, \Delta f_s^{\max}) \quad (13)$$

Therefore, more OFLs will participate in FRS with the increase of the system frequency deviation, which is similar with the response effectiveness in CCM. In order to avoid the frequent schedule of one specific OFL, the thresholds are allocated again after each round of dispatch.

As for the CFLs, the terminal controllers preset the system frequency deviation ranges, Δf_s^{\min} and Δf_s^{\max} . When the system frequency deviation occurs, the terminal controllers will adjust the CFLs' operating frequency based on Eq. (14).

$$f_{CFL,j}^{ADJ}(\Delta f_{TC,j}(t)) = \begin{cases} f_{CFL,j}(t), & \Delta f_{TC,j}(t) \leq \Delta f_s^{\min} \\ f_{CFL,j}(t) - \frac{\Delta f_{TC,j}(t) - \Delta f_s^{\min}}{\Delta f_s^{\max} - \Delta f_s^{\min}} \Delta f_s^{\min} & \Delta f_s^{\min} \leq \Delta f_{TC,j}(t) \leq \Delta f_s^{\max} \\ (f_{CFL,j}(t) - f_{CFL,j}^{\min}), & \\ f_{CFL,j}^{\min}, & \Delta f_{TC,j}(t) \geq \Delta f_s^{\max} \end{cases} \quad (14)$$

In summary, the DCM algorithm in the terminal controllers can realize the same response effectiveness with the CCM algorithm in the control centre. The main differences of the two control frameworks are the CML and the FDE, where the CML in CCM is large but small in DCM, while the FDE in CCM is small but large in DCM.

(3) System frequency response model of the distributed control method

Fig. 5 shows the system frequency response model of the DCM, where the main difference with the CCM is the measurement method of the system frequency deviation. The system frequency is monitored by each terminal controller in the DCM, which is expressed as $\Delta f_{TC,i}$.

Based on Eqs. (1)–(4) and (12)–(14), the regulation power of the OFLs and the CFLs in the DCM can be expressed as

$$\Delta P_{OFL,total} = -P_{OFL,r,avg} \sum_{i=1}^N [\Delta f_{TC,i} - \Delta f_{OFL,i}^{THR}] \quad (15)$$

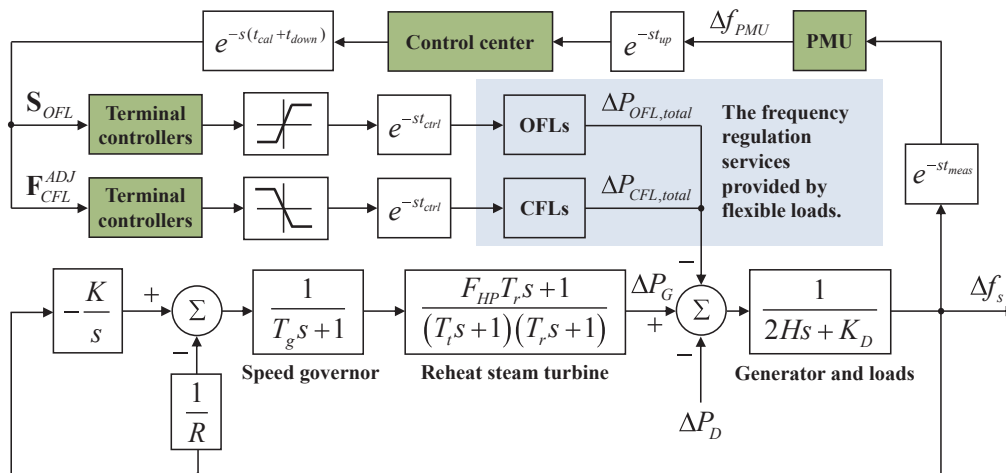


Fig. 3. The system frequency response model of the centralized control method.

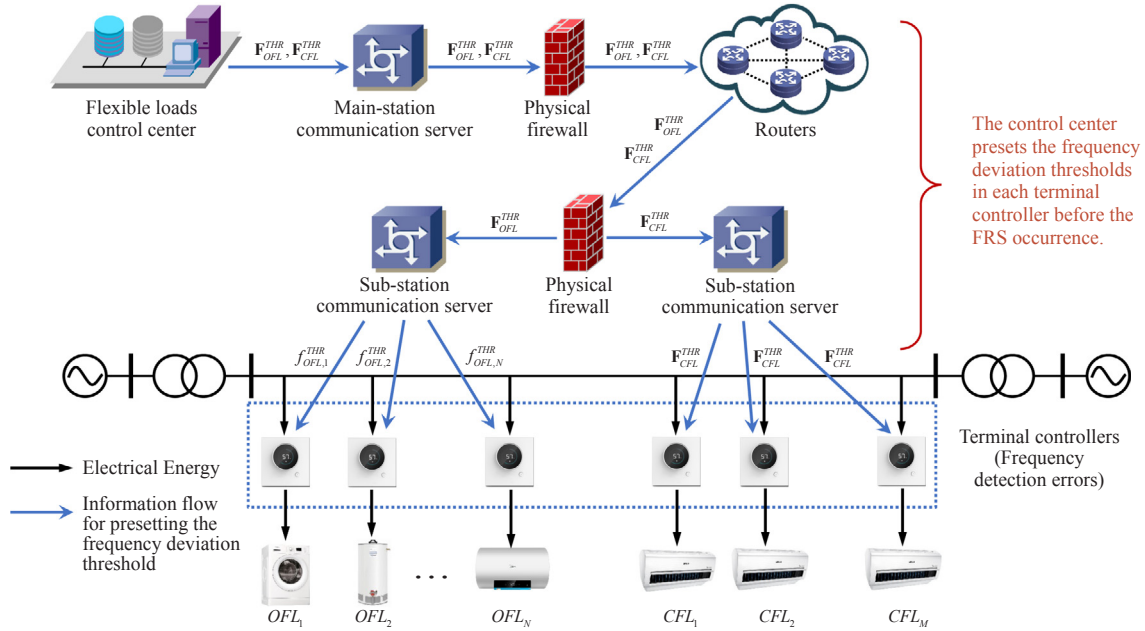


Fig. 4. The framework of the distributed control method.

$$\Delta P_{CFL,total} = \mathbf{K}_{CFL}^T (\mathbf{F}_{CFL}^{ADJ} - \mathbf{F}_{CFL}) \quad (16)$$

where the ceiling function $[\Delta f_{TC,i} - \Delta f_{OFL,i}^{THR}]$ is equal to 1 when the $\Delta f_{TC,i}$ is larger than the threshold value $\Delta f_{OFL,i}^{THR}$. However, the measured system frequency deviation $\Delta f_{TC,i}$ may be not accuracy and cause regulation power errors, especially with the increasing number of FLs. In Section 4, a hybrid control method (HCM) is proposed to decrease the FDE.

4. Framework and implementation procedure of the hybrid control method

(1) Framework of the hybrid control method

Fig. 6 shows the control framework of the hybrid control method (HCM) and the system frequency response model. It can be seen that the PMU is installed on the power system and can monitor the system frequency deviation, just as that in CCM. Moreover, the terminal controllers of FLs can also measure the system frequency deviation locally, similar with that in DCM. The terminal controllers can take action based on the local frequency detection values ($\Delta f_{TC,i}$), so that the CML in CCM can be avoided. However, as mentioned above, the $\Delta f_{TC,i}$ may have

FDE and cause response power bias. To address this problem, a modification model of $\Delta f_{TC,i}$ for decreasing the FDE is developed based on the historical statistical data of FDEs. The $\Delta f_{TC,i}$ is modified to $\hat{\Delta f}_{TC,i}$ before implementing the control algorithm in Eqs. (13) and (14). After the control process, the measured system frequency deviation by the PMU will be transmitted to the terminal controllers, which is regard as the accuracy value and will be compared with $\Delta f_{TC,i}$ to adjust the parameters of the modification model. In this manner, the correcting precision of $\Delta f_{TC,i}$ can be raised with the increase of measured data.

(2) Modification model of the terminal controllers

The measured system frequency deviation by the PMU (Δf_{PMU}) is regard as the accuracy value, so that the FDE can be defined as

$$\Delta f_{e,i,k} = \Delta f_{PMU,k} - \Delta f_{TC,i,k} \quad (17)$$

where $k = 1, 2, \dots, K$ is the total number of historical data of the controller- i . Based on the generalized error distribution theory, the FDEs are assumed to obey the normal distribution, which is expressed as

$$X_i \sim N(\mu_i, \sigma_i^2) \quad (18)$$

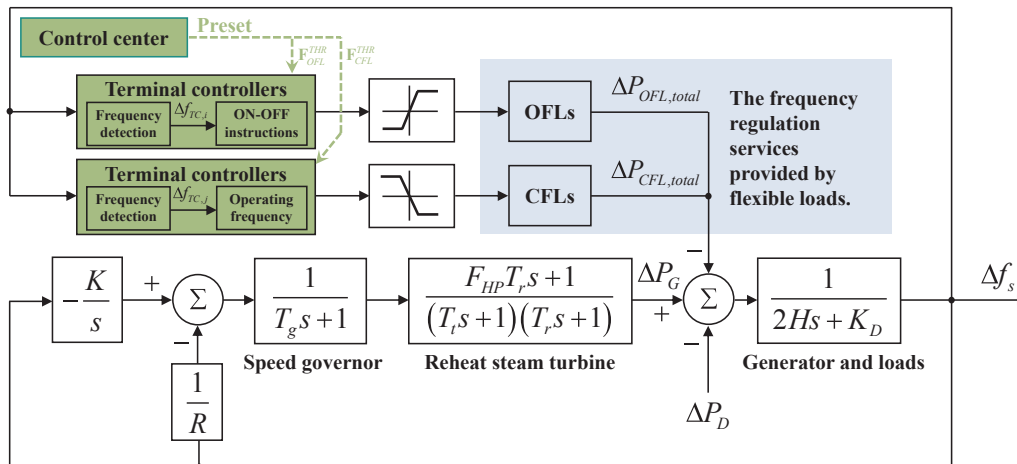


Fig. 5. The system frequency response model of the distributed control method.

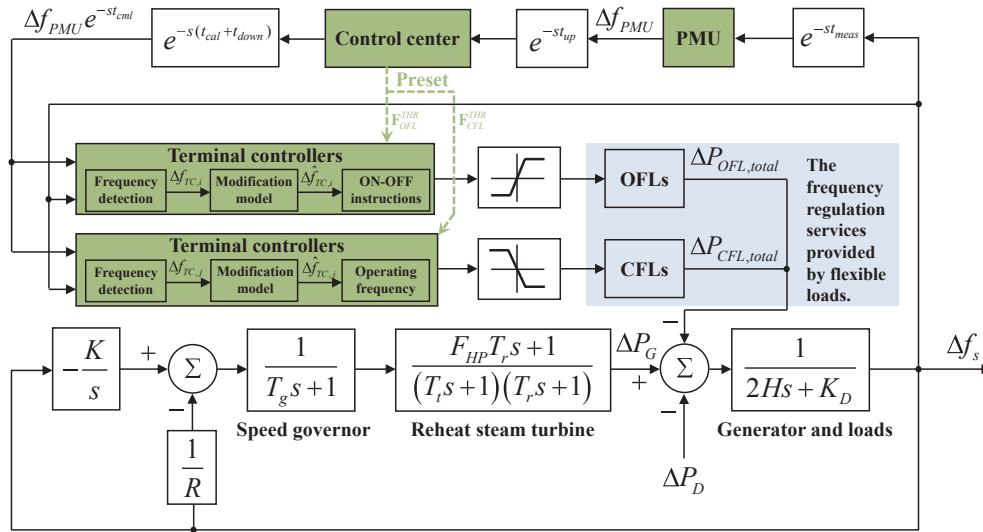


Fig. 6. The system frequency response model of the hybrid control method.

where μ_i and σ_i^2 are the FDE distribution expectation and variance of the terminal controller- i . X_i is the statistical set of $\Delta f_{e,i,k}$, which can be described as $X_i = \{\Delta f_{e,i,1}, \Delta f_{e,i,2}, \dots, \Delta f_{e,i,K}\}$.

However, the ideal values of the μ_i and σ_i^2 are unknown, and have to be estimated based on the historical statistical data. Cramér-Rao bound provides a lower bound on the variance of unbiased estimators aiming at deterministic (though unknown) parameters [43]. Therefore, the minimum-variance unbiased estimator (MVUE) of μ_i and σ_i^2 can be calculated as

$$E_i = \frac{1}{K} \sum_{k=1}^K \Delta f_{e,i,k} \quad (19)$$

$$S_i^2 = \frac{1}{K-1} \sum_{k=1}^K (\Delta f_{e,i,k} - E_i)^2 \quad (20)$$

Then, the modified system frequency deviation $\Delta \hat{f}_{TC,i}$ can be calculated as

$$\Delta \hat{f}_{TC,i} = \Delta f_{TC,i} + \xi_i \quad (21)$$

where ξ_i obeys $N(E_i, S_i^2)$. Moreover, considering the calculation methods in Eqs. (19) and (20) may need large storage space for the historical data and high performance chip for the computation, a simplified iterative approach is proposed to update the two parameters E_i and S_i^2 .

Suppose the new round measurement data of the system frequency deviation is $\Delta f_{e,i,K+1}$. Then, we have the updated expectation \hat{E}_i , which is expressed as

$$\begin{aligned} \hat{E}_i &= \frac{1}{K+1} \sum_{k=1}^{K+1} \Delta f_{e,i,k} = \frac{1}{K+1} (\sum_{k=1}^K \Delta f_{e,i,k} + \Delta f_{e,i,K+1}) \\ &= \frac{K}{K+1} \left(\frac{1}{K} \sum_{k=1}^K \Delta f_{e,i,k} \right) + \frac{1}{K+1} \Delta f_{e,i,K+1} = \frac{K}{K+1} E_i + \frac{1}{K+1} \Delta f_{e,i,K+1} \end{aligned} \quad (22)$$

Similarly, the updated variance \hat{S}_i^2 for the $(K+1)$ sets of measurement data can be expressed as

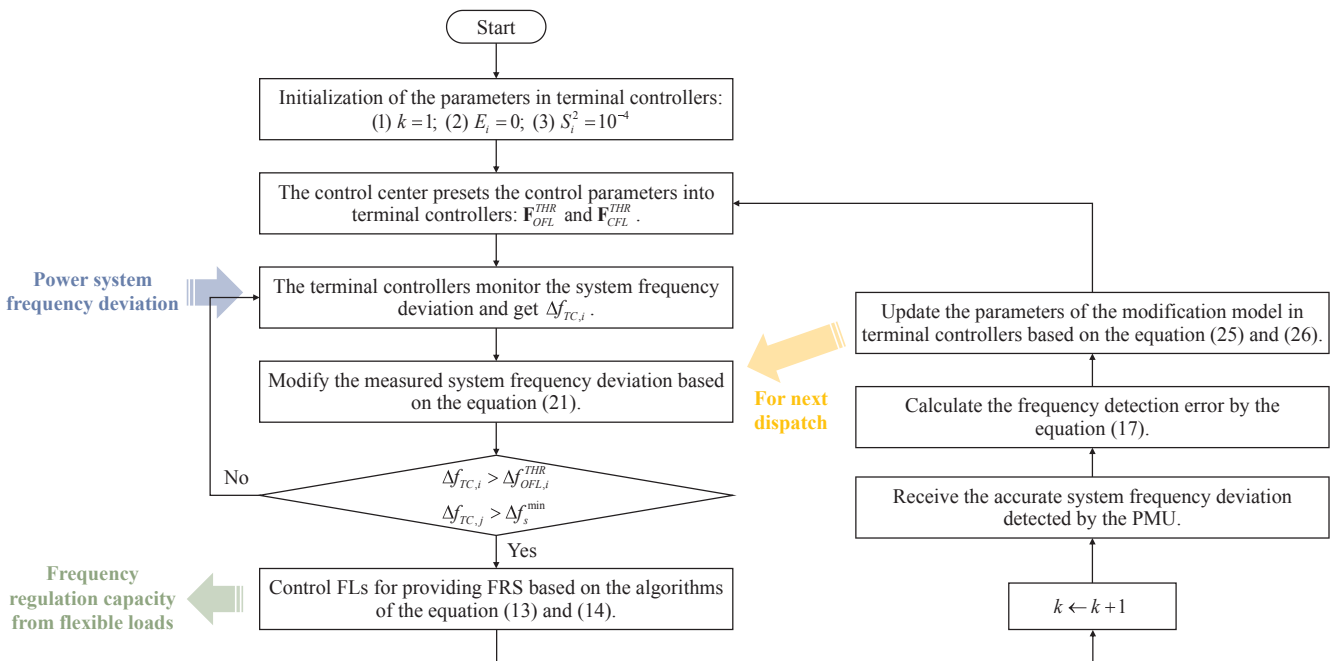


Fig. 7. The implementation procedure of the hybrid control method.

$$\begin{aligned}
 \hat{S}_i^2 &= \frac{1}{K} \sum_{k=1}^{K+1} (\Delta f_{e,i,k} - \hat{E}_i)^2 = \frac{1}{K} \left[\sum_{k=1}^K (\Delta f_{e,i,k} - \hat{E}_i)^2 + (\Delta f_{e,i,K+1} - \hat{E}_i)^2 \right] \\
 &= \frac{1}{K} \sum_{k=1}^K [(\Delta f_{e,i,k} - E_i) + (E_i - \hat{E}_i)]^2 + \frac{1}{K} (\Delta f_{e,i,K+1} - \hat{E}_i)^2 \\
 &= \frac{1}{K} \sum_{k=1}^K [(\Delta f_{e,i,k} - E_i)^2 + 2(E_i - \hat{E}_i)(\Delta f_{e,i,k} - E_i) + (E_i - \hat{E}_i)^2] \\
 &\quad + \frac{1}{K} (\Delta f_{e,i,K+1} - \hat{E}_i)^2 \\
 &= \frac{1}{K} \sum_{k=1}^K (\Delta f_{e,i,k} - E_i)^2 + 2(E_i - \hat{E}_i) \left(\frac{1}{K} \sum_{k=1}^K \Delta f_{e,i,k} - E_i \right) + (E_i - \hat{E}_i)^2 \\
 &\quad + \frac{1}{K} (\Delta f_{e,i,K+1} - \hat{E}_i)^2
 \end{aligned} \tag{23}$$

Since $E_i = \frac{1}{K} \sum_{k=1}^K \Delta f_{e,i,k}$, then Eq. (23) can be derived into

$$\begin{aligned}
 \hat{S}_i^2 &= \frac{1}{K} \sum_{k=1}^K (\Delta f_{e,i,k} - E_i)^2 + (E_i - \hat{E}_i)^2 + \frac{1}{K} (\Delta f_{e,i,K+1} - \hat{E}_i)^2 \\
 &= \frac{K-1}{K} \cdot \frac{1}{K-1} \sum_{k=1}^K (\Delta f_{e,i,k} - E_i)^2 + (E_i - \hat{E}_i)^2 + \frac{1}{K} (\Delta f_{e,i,K+1} - \hat{E}_i)^2 \\
 &= \frac{K-1}{K} S_i^2 + (E_i - \hat{E}_i)^2 + \frac{1}{K} (\Delta f_{e,i,K+1} - \hat{E}_i)^2
 \end{aligned} \tag{24}$$

Therefore, Eqs. (19) and (20) can be transformed into

$$\hat{E}_i = \frac{K-1}{K} E_i + \frac{1}{K} \Delta f_{e,i,K} \tag{25}$$

$$\hat{S}_i^2 = \frac{K-2}{K-1} S_i^2 + (E_i - \hat{E}_i)^2 + \frac{1}{K-1} (\Delta f_{e,i,K} - \hat{E}_i)^2 \tag{26}$$

In this manner, the terminal controller only needs to store two parameters (E_i and S_i^2), instead of all the $\Delta f_{e,i,k}$ data in history.

(3) Implementation procedure of the hybrid control method

Fig. 7 shows the implementation procedure of the HCM. The first step is the initialization of the parameters in the terminal controllers.

Then, the control centre presets the control parameters into the terminal controllers, including the frequency deviation thresholds $\Delta f_{OFL,i}^{THR}$ for OFLs and the frequency deviation response ranges (Δf_s^{\min} and Δf_s^{\max}) for CFLs. The terminal controllers monitor the system frequency and will adjust the operating states of the corresponding FLs, if the deviation value exceeds the threshold. After the regulation, the parameters of the modification model will be updated for the next round of dispatch.

5. Case studies and discussions

5.1. The test system

The test system adopts the power systems in Figs. 3, 5 and 6 for the CCM, DCM and HCM, respectively. The power systems include the reheat steam generator, the conventional unchangeable loads, and FLs (OFLs and CFLs). The parameters of the FLs are based on the actual test data in [15] and [16], where the OFLs are assumed to be the typical heating, ventilating and air conditioning (HVAC) systems, and the CFLs are assumed as the inverter air conditioners (IAC). The ambient temperature and the model parameters are based on the test data and the national standards in Hangzhou, China, on August 1st, 2015 [15]. The set temperatures of the HVACs and IACs are distributed randomly between 22 °C and 26 °C to simulate various requirements of the room temperatures for different customers [44]. The frequency regulation ranges of CFLs are 1 ~ 150 Hz [16]. The coefficients of the CFLs $\kappa_{CFL,j}$ and $l_{CFL,j}$ are 0.04 kW/Hz and 0.02 kW, respectively. The average operating power of the OFLs and CFLs are around 1 kW and 1.4 kW, respectively. It is assumed that the number of OFLs and CFLs are 10,000 in the power system.

The generation capacity of the reheat steam generator is 800 MW

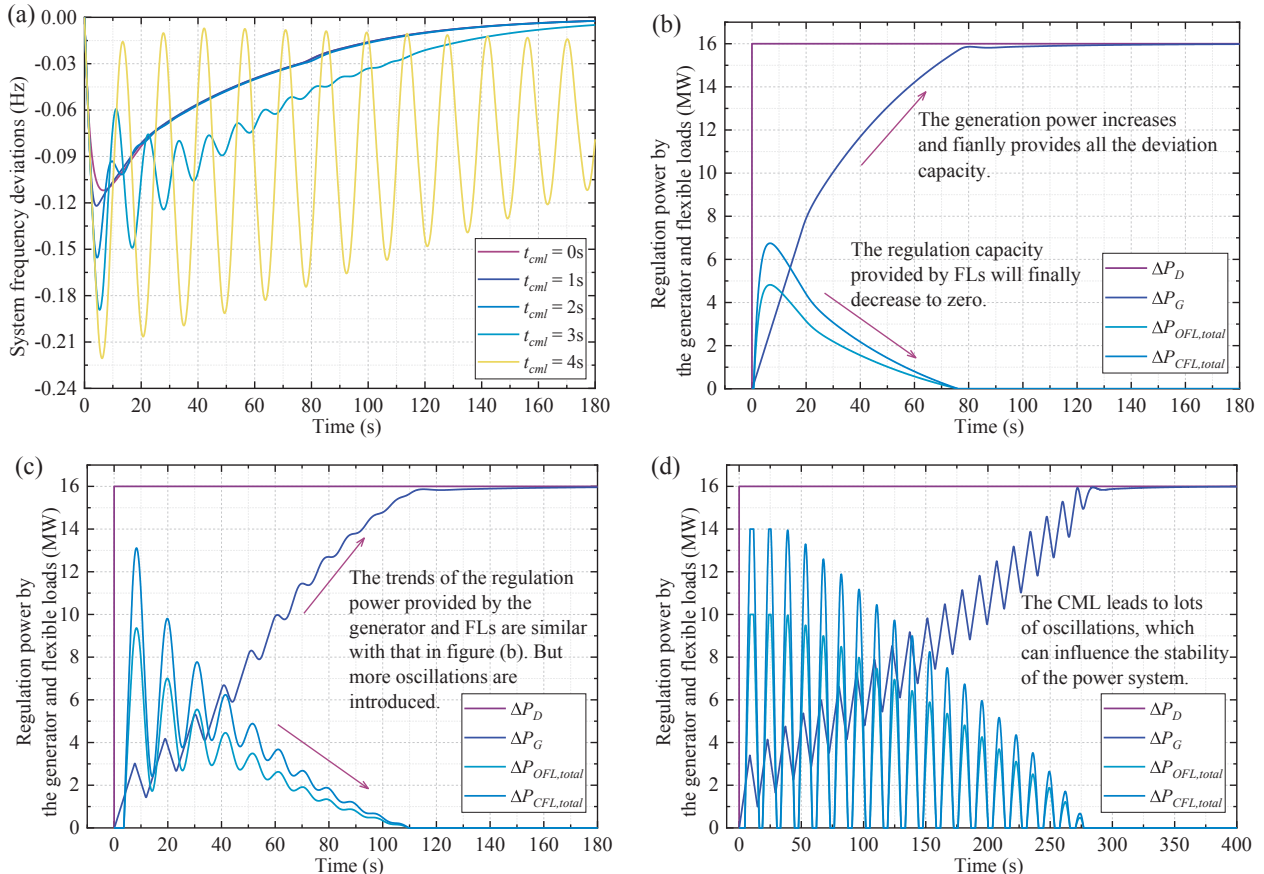


Fig. 8. The frequency deviations and regulation powers of the power system based on the centralized control method: (a) the frequency deviations with different CMLs; (b) the regulation power when CML is 0 s; (c) the regulation power when CML is 3 s; (d) the regulation power when CML is 4 s.

[16,41,45]. The time constants of the speed governor (T_g), the turbine (T_t), and the reheat process (T_r) are 0.2 s, 0.3 s and 7 s, respectively. The high pressure turbine's power fraction (F_{HP}), the speed droop parameter (R), and the integral gain (K) are 0.3, 0.05 and 0.5, respectively. Moreover, the ramp rate constraint of the generator must be considered in practice, which is set as 3% per minute [41]. The generator inertia (H) and the load-damping factor (K_D) are 10 and 1, respectively. The rated frequency of the power system is 50 Hz. The minimum and maximum frequency deviation thresholds are $\Delta f_s^{\min} = 0.03$ Hz and $\Delta f_s^{\max} = 0.2$ Hz, respectively. It is assumed that the disturbance load ΔP_D is 2% of the system capacity (i.e., $\Delta P_D = 16$ MW).

5.2. Case 1: The analysis of the communication latency

Fig. 8 shows the system frequency deviations in five scenarios, including $t_{cml} = 0$ s, $t_{cml} = 1$ s, $t_{cml} = 2$ s, $t_{cml} = 3$ s, and $t_{cml} = 4$ s. It can be seen that the frequency oscillations are not apparent, when the CML is less than 2 s. However, the oscillations will be obvious when CML is equal to or larger than 3 s, which can result in the increase of the maximum frequency deviation (MFD) and the extension of the recovery time (RT). The RT is defined as the time interval from the occurrence moment of the frequency deviation to the moment when the deviation returns to the dead band value, which is ± 0.03 Hz. The MFD, RT, the maximum regulation powers of OFLs and CFLs are presented in Table 1. The MFD and RT are similar when the CML is less 2 s. However, when the CML is 4 s, the MFD and RT will increase to -0.221 Hz and 272.9 s, respectively, which are around twice the corresponding values in the $t_{cml} = 1$ s scenario.

Fig. 8(b)–(d) shows the regulation power provided by the generator and FLs when the CML is 0 s, 3 s, and 4 s, respectively. In Fig. 8(b), the regulation powers of the OFLs and CFLs increase first, and then decrease to zero finally. Because the FLs will restore to the original operating states with the recovery of the system frequency. The regulation power of the generator increases smoothly and finally provides all the disturbance load. In Fig. 8(c) and (d), the regulation power oscillations are obvious, which is harmful to the generator and can lead to more influences on the operation sates of FLs. In these scenarios, the comfort of customers and even the service life of some appliances may be impacted. Moreover, as shown in Table 1, the maximum regulation power by FLs rises with the increase of the CML. Because longer CMLs result in larger system frequency deviations, which makes more FLs reach the DR threshold values to take action.

Fig. 9 shows the system frequency deviations under different available regulation capacities from FLs, where the CML is assumed as a constant (i.e., 2 s). If there is no FLs, the MFD is around -0.45 Hz, while the MFD can be decreased to -0.18 Hz when there are 5,000 OFLs and CFLs. From this perspective, the FLs can assist in decreasing the system frequency fluctuations significantly. Because the FLs have less inertia and can take action faster than traditional generation units (e.g., the reheat steam generator).

However, as shown in Fig. 9(b), the frequency oscillations appear during the regulation process and will be more obvious with the increase of the FLs' number. Considering the scenarios in Fig. 9 are under the same CML, the results illustrate that larger FLs' capacities are more sensitive to the CML. Moreover, the MFD cannot decrease significantly anymore, even though there are more FLs. Therefore, due to the CML, the regulation effectiveness of FLs cannot be increased with more FLs, and even can lead to a deterioration effect. In summary, the CML should be considered more with discretion in the power systems with large-scale FLs, which is exactly the challenge in the near future smart grid.

5.3. Case 2: The analysis of the system frequency detection error

The system frequency is measured by the terminal controllers in the DCM, which may be not as accurate as that in CCM by the PMU. The FDEs of the terminal controllers are shown in Fig. 10, which are used to

illustrate the impact of the FDE on the regulation effectiveness of FLs. The disturbance load ΔP_D and the number of FLs are the same with that in Case 1, which are 16 MW and 10,000, respectively.

Fig. 11(a) shows the system frequency deviations when the terminal controllers are with and without FDE. There are two main negative influences. One is some small jitters are introduced by the FDE during the frequency recovery process. The other one is the MFD becomes larger, which changes from -0.112 Hz to -0.120 Hz. Fig. 11(b) shows the system frequency deviations with different available capacities of FLs in DCM. Compared with the scenario without FLs in Fig. 9(a), the system frequency deviations are decreased significantly from -0.453 Hz to -0.171 Hz ($N = M = 5000$), which relies on the small inertia of FLs to take action rapidly.

Moreover, it can be seen from the Fig. 11(b) that the FDE in DCM will not bring large oscillations, even though the number of FLs reaches 20,000. However, as shown in Fig. 8(a), the CML in CCM will introduce serious oscillations. Especially with the increasing number of FLs, the CML can cause more oscillations, as shown in Fig. 9(b). Therefore, faced with large-scale FLs in the future smart grid, the constraint on the CML should be smaller to avoid the serious frequency oscillations, while exactly the CML may be longer with larger number of FLs. From this perspective, the DCM is more appropriate for large-scale FLs than the CCM.

The MFD, RT, the maximum regulation powers of OFLs and CFLs in Case 2 are presented in Table 2. With the increasing number of FLs, more regulation capacities are provided by the OFLs and CFLs, so that the MFD and RT are decreased. Moreover, the positive effect of FLs is significant at the beginning stage, while the effect will be unobvious gradually with the increasing number of FLs, because the available capacity of FLs becomes large enough to deal with the disturbance power ΔP_D .

5.4. Case 3: The effectiveness of the proposed hybrid control method

On the basis of the control structure in Fig. 6 and the implementation procedure in Fig. 7, the system frequency deviations are measured and then modified by terminal controllers locally. As shown in Eqs. (17)–(26), the modification method of the measured frequency detections ($\Delta f_{TC,i}$) by terminal controllers is based on the historical data of FDEs. Therefore, the modification precision can be improved with the number of data, i.e., the response times. The FDEs of the terminal controllers are assumed to be the same with that in DCM, as shown in Fig. 10. The disturbance load ΔP_D , the number of FLs, and the sampling frequency of terminal controllers are 16 MW, 10,000, and 1 s, respectively.

Fig. 12 shows the results of the frequency regulation by the HCM, where Fig. 12(a) and (b) are the fifth and tenth response, respectively. The ideal frequency regulation results are the first scenario, which is without FDE. The actual regulation results are the second scenario, which is with FDE but without modification of the measured frequency deviation value. The third scenario shows the effectiveness of the modification method in HCM.

It can be seen from Fig. 12 that the MFD and the RT can be decreased and get close to the ideal curves by the HCM. The ideal MFD is -0.112 Hz, while it will be -0.120 Hz if the terminal controllers have

Table 1
The results with different communication latencies in Case 1.

Scenarios	MFD (Hz)	RT (s)	$\Delta P_{OFL,total}^{\max}$ (MW)	$\Delta P_{CFL,total}^{\max}$ (MW)	Oscillations
$t_{cml} = 0$ s	-0.112	75.8	0	0	Non-obvious
$t_{cml} = 1$ s	-0.122	75.8	5.41	7.57	Non-obvious
$t_{cml} = 2$ s	-0.155	76.7	7.38	10.33	Non-obvious
$t_{cml} = 3$ s	-0.189	106.8	9.36	13.11	Obvious
$t_{cml} = 4$ s	-0.221	272.9	10	14	Obvious

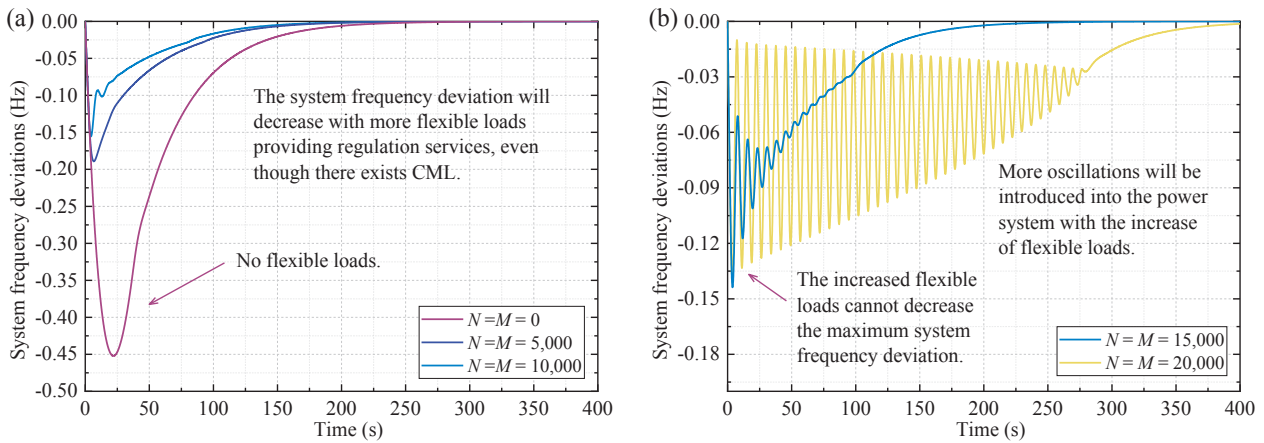


Fig. 9. The frequency deviations of the power system based on the centralized control method with different available capacities of flexible loads.

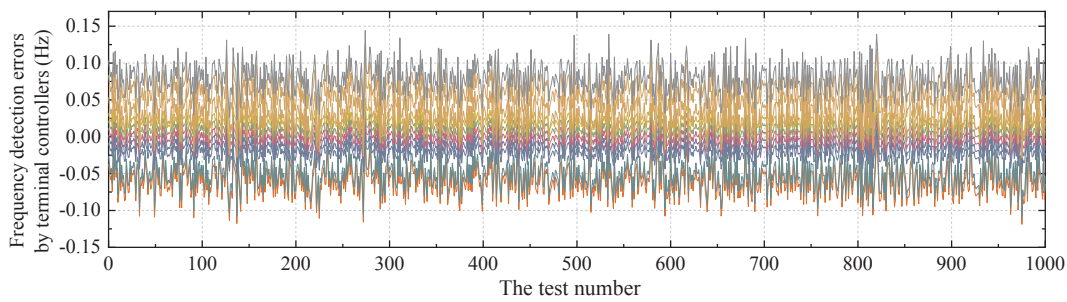


Fig. 10. The frequency detection errors of the terminal controllers.

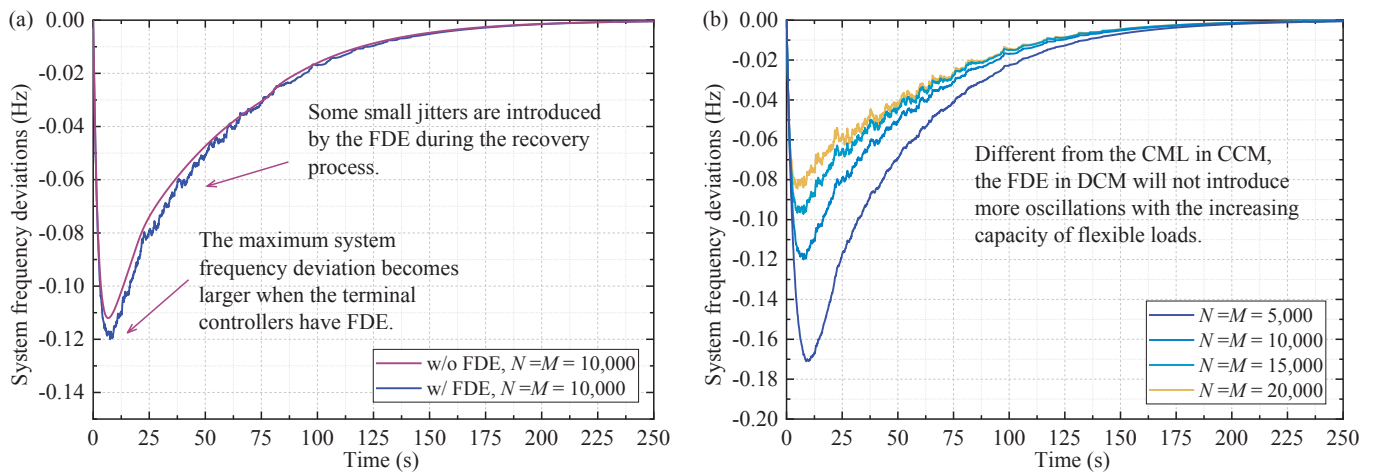


Fig. 11. The frequency deviations of the power system based on the distributed control method: (a) the comparison of the frequency regulation process with and without FDE; (b) the scenarios with different available capacities of flexible loads.

Table 2
The results with different number of flexible loads considering FDE in Case 2.

Scenarios	MFD (Hz)	RT (s)	$\Delta P_{OFL,total}^{max}$ (MW)	$\Delta P_{CFL,total}^{max}$ (MW)	Oscillations
$N = M = 0$	-0.453	134.5	0	0	Non-obvious
$N = M = 5000$	-0.171	89.2	5.00	7.00	Non-obvious
$N = M = 10,000$	-0.120	75.8	6.97	9.76	Non-obvious
$N = M = 15,000$	-0.097	72.6	8.59	12.02	Non-obvious
$N = M = 20,000$	-0.084	68.4	10.02	14.03	Non-obvious

FDEs. The MFD is modified from -0.120 Hz to -0.116 Hz in the fifth response and -0.110 Hz in the tenth response, which are closer to the ideal value. The modified RT is also shortened from 75.4 s in the fifth response to 74.6 s in the tenth response. Therefore, the results illustrate that the modification performance can be improved with the increase of the response times. The measured results are shown in detail in Table 3.

The FDE ($\Delta f_{e,i,k}$) defined in Eq. (17) are counted in ten response times, where the statistical data of the terminal controller- i are shown in Fig. 13(a). The fitting curve shows that the normal distribution can fit well on the statistical data of FDEs. The distribution expectation (μ_i) and the variance (σ_i^2) are 0.01002 and 0.00996^2 , respectively. Fig. 13(b) shows the normal quantile-quantile plot (Q-Q plot) of the statistical data, which can be used to check the normality assumption of

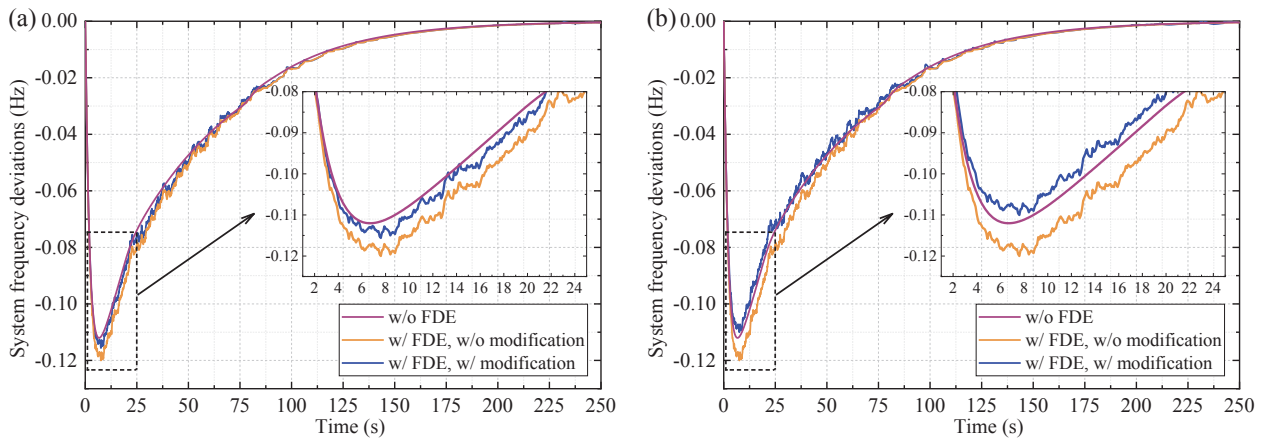


Fig. 12. The comparisons of the system frequency deviations based on the hybrid control method: (a) the fifth response; (b) the tenth response.

Table 3

The results with different disturbance powers in the hybrid control method.

ΔP_D (MW)	scenarios	MFD (Hz)	RT (s)	$\Delta P_{OFL,total}^{max}$ (MW)	$\Delta P_{CFL,total}^{max}$ (MW)
8	w/o FDE	-0.063	35.3	0	0
	w/ FDE, w/o modification	-0.069	35.7	3.96	5.55
	w/ FDE, w/ modification	-0.063	34.1	4.22	5.86
16	w/o FDE	-0.112	76.1	0	0
	w/ FDE, w/o modification	-0.120	75.8	6.97	9.76
	w/ FDE, w/ modification	-0.110	74.6	6.65	10.12
	w/ FDE, w/ modification-5th	-0.116	75.4	7.18	9.50
24	w/o FDE	-0.161	103.3	0	0
	w/ FDE, w/o modification	-0.169	104.0	9.88	13.83
	w/ FDE, w/ modification	-0.161	103.8	9.92	13.93
32	w/o FDE	-0.228	125.3	0	0
	w/ FDE, w/o modification	-0.234	125.5	10.00	14.00
	w/ FDE, w/ modification	-0.227	125.1	10.00	14.00
40	w/o FDE	-0.484	170.0	0	0
	w/ FDE, w/o modification	-0.486	168.9	10.00	14.00
	w/ FDE, w/ modification	-0.485	170.4	10.00	14.00

Here “w/” means “with”, “w/o” means “without”.

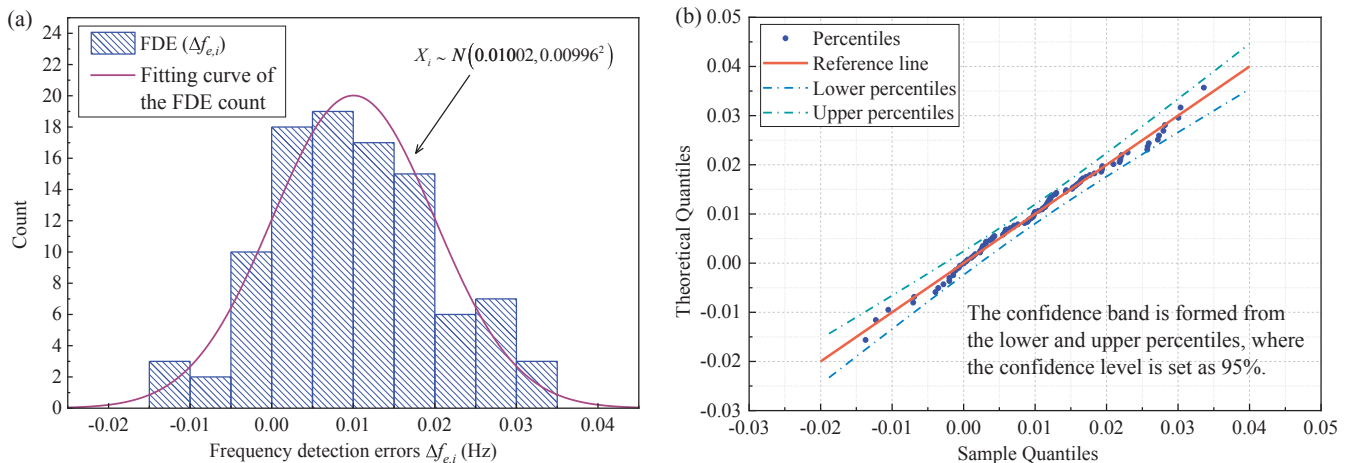


Fig. 13. The fitting curve of the frequency detection errors: (a) the statistical data and corresponding fitting curve; (b) the quantile–quantile plot of the statistical data.

the statistical data. The percentile points will fall on the reference line (i.e., a 45 degree angle line), if the FDEs obey the normal distribution. The confidence level is set as 95%, which forms the confidence band in the Fig. 13(b). It can be seen that most of the points fall on the reference line, and all of the points are in the confidence band. Apart from the

graphical method (i.e., Q-Q plot), some numerical methods have also been proposed to check the normality assumption, including the Shapiro-Wilk (SW) test, Kolmogorov-Smirnov (KS) test, Anderson-Darling (AD) test, and Lilliefors (LF) test [46]. The corresponding p-values are 0.72715, 1.000, 0.65682, and 0.200, respectively. Since all the p-values

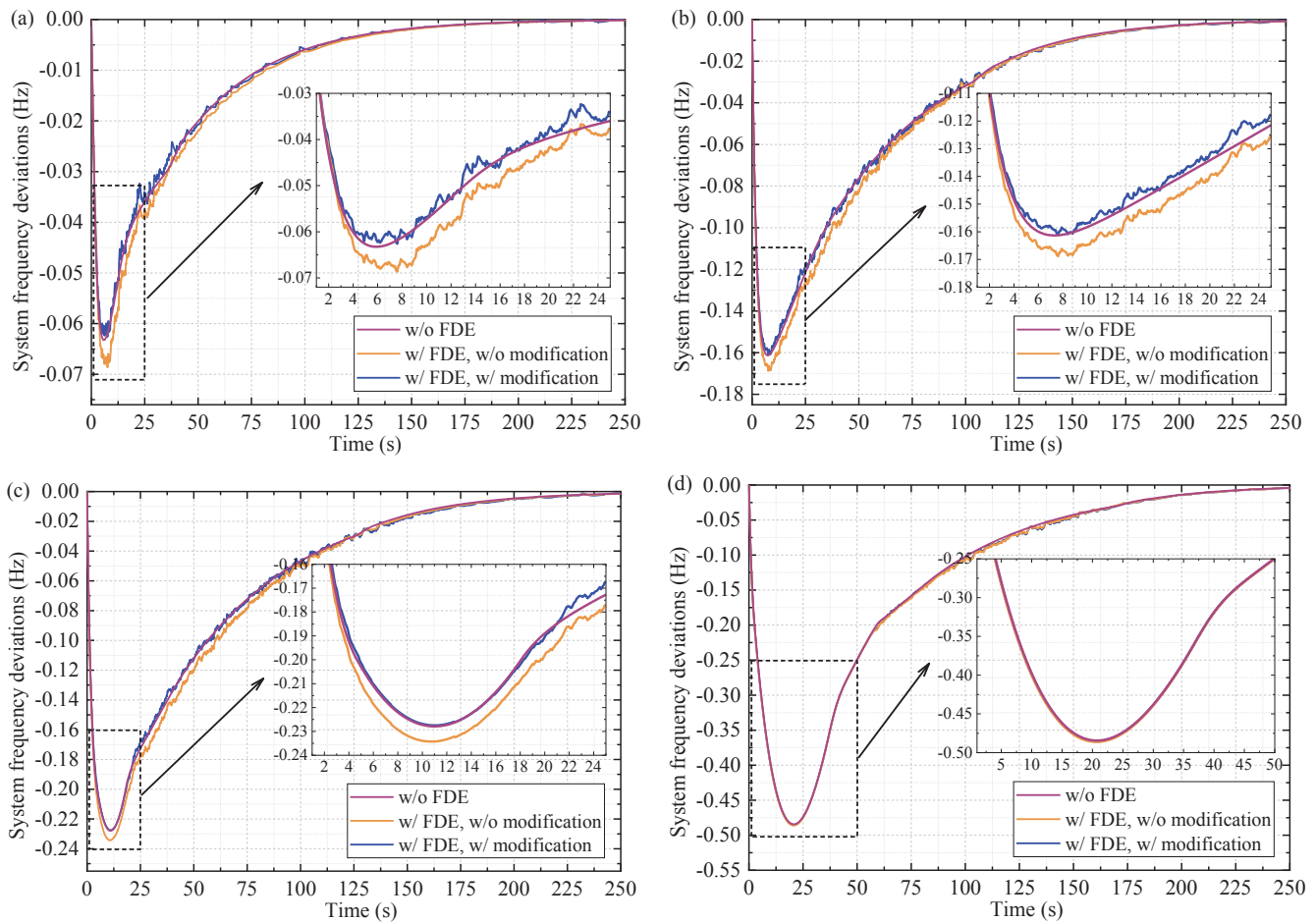


Fig. 14. The comparisons of the system frequency deviations based on the hybrid control method under different disturbance powers: (a) 8 MW; (b) 24 MW; (c) 32 MW; (d) 40 MW.

are larger than 0.05, it can be concluded that the statistical data of FDEs obeys the normal distribution at the level of significance.

The influence of different disturbance powers on the effectiveness of the proposed HCM is also illustrated, as shown in Fig. 14. The number of FLs are the same (10,000), which means the scenarios are with the same available regulation capacity from FLs. The sampling frequency and the response times of terminal controllers are 1 s and 10, respectively. The disturbance powers in Fig. 14(a)–(d) are set to be 8 MW (1%), 24 MW (3%), 32 MW (4%), and 40 MW (5%), respectively. Fig. 12(b) shows the scenario with 16 MW (2%) disturbance power.

Based on the Fig. 14 and Table 3, it can be seen that the MFD will be larger and the RT will be longer with the increase of the disturbance power. That is because the regulation speed of the generator and the available regulation capacity of the FLs are the same in these scenarios, where the MFD and RT will be worsen with larger disturbance power. Moreover, the maximum dispatched regulation powers of FLs are increased from $\Delta P_{OFL, total}^{max} = 4.22$ MW and $\Delta P_{CFL, total}^{max} = 5.86$ MW in $\Delta P_D = 8$ MW scenario to the upper limits ($\Delta P_{OFL, total}^{max} = 10.00$ MW and $\Delta P_{CFL, total}^{max} = 14.00$ MW) in larger disturbance power scenarios. As shown in Fig. 14(d), the increased disturbance power causes the overlap of the three curves. Because the system frequency deviations are too large in this scenario, and all the regulation capacities are dispatched. In this condition, the FDE can be ignored and the modification method in HCM is meaningless. The only and fundamental solution is to increase the available regulation capacities provided by FLs or generators.

6. Conclusions

This paper proposes a novel hybrid control method (HCM) to compensate the communication latency (CML) and the frequency detection error (FDE) during the control process of flexible loads (FLs) for providing frequency regulation service (FRS) in power systems. Firstly, the aggregation models of the ON-OFF FLs (OFLs) and continuously adjustable FLs (CFLs) are both developed and controlled in this paper. The CFLs are increasing rapidly nowadays (e.g., the inverter air conditioners), and proved to be more flexible and suitable to provide FRS. However, the CFLs are rarely considered in the previous studies, which mainly pay attention to the OFLs. Moreover, the framework, control algorithm and the system model of the centralized control method (CCM) and distributed control method (DCM) are developed, respectively, which consider the influence of the CML and FDE. On this basis, the HCM based on the CCM and DCM is proposed to compensate the CML and FDE, in which the modification method of FDE is developed for improving the estimation accurate of the system frequency deviations. The simplified iterative approach for updating the parameters in the FDE modification model is proposed to decrease the requirement on the data storage space and computation of the terminal controllers.

The numerical studies show that the effectiveness of the FRS provided by FLs can be impacted significantly by the CML and FDE, especially with the increase available regulation capacity of FLs. The maximum frequency deviation (MFD) and the recovery time (RT) will be extended from -0.112 Hz and 75.8 s to -0.221 Hz and 272.9 s, respectively, if the CML reaches 4 s. Moreover, the large number of FLs can lead to significant system frequency oscillations during the

regulation process due to the CML, which will be a serious problem in the power systems. Apart from the influence of the CML, the MFD is also extended from -0.112 Hz to -0.120 Hz as a result of the FDE. Faced with this challenge, the results in numerical studies illustrate that the HCM can avoid the CML and reduce the FDE. The MFD is modified to -0.116 Hz in the fifth response and -0.110 Hz in the tenth response, which are almost equal to the ideal value (-0.112 Hz) when there is no CML and FDE. Besides, the modified frequency deviation curves can be nearly overlapped with the ideal regulation curves. Therefore, this proposed models and methods can compensate the CML and FDE well, which are useful for guiding the DR projects in the future smart grid.

Acknowledgements

This work is supported in part by the National Key Research and Development Program of China under Grant 2016YFB0901100, and in part by the National Natural Science Foundation of China (NSFC) under Grant 51577167.

References

- [1] U.S. News. Tens of millions in northern Brazil hit by massive power outage; 2018. <https://www.reuters.com/article/us-brazil-power/tens-of-millions-in-northern-brazil-hit-by-massive-power-outage-idUSKBN1GX3CN/>.
- [2] Executive Yuan, Taiwan. Administrative investigation report on the 815 power failure; 2017. <https://www.eiy.gov.tw/Page/9277F759E41CCD91/8e438787-698f-478a-b17b-fa747d321e14/>.
- [3] Rebours YG, Kirschen DS, Trotignon M, Rossignol S. A survey of frequency and voltage control ancillary services—Part I: Technical features. *IEEE Trans Power Syst* 2007;22(1):350–7.
- [4] Wang J, Zhong H, Ma Z, Xia Q, Kang C. Review and prospect of integrated demand response in the multi-energy system. *Appl Energy* 2017;15(202):772–82.
- [5] Ding Y, Shao C, Yan J, Song Y, Zhang C, Guo C. Economical flexibility options for integrating fluctuating wind energy in power systems: the case of China. *Appl Energy* 2018;15(228):426–36.
- [6] Wang Y, Gan D, Sun M, Zhang N, Lu Z, Kang C. Probabilistic individual load forecasting using pinball loss guided LSTM. *Appl Energy* 2019;1(235):10–20.
- [7] Siano P. Demand response and smart grids—a survey. *Renew Sustain Energy Rev* 2014;30:461–78.
- [8] Cui W, Ding Y, Hui H, Lin Z, Du P, Song Y, et al. Evaluation and sequential dispatch of operating reserve provided by air conditioners considering lead-lag rebound effect. *IEEE Trans Power Syst* 2018;33(6):6935–50.
- [9] Vardakas JS, Zorba N, Verikoukis CV. A survey on demand response programs in smart grids: pricing methods and optimization algorithms. *IEEE Commun Surv Tutor* 2015;17(1):152–78.
- [10] Albadi MH, El-Saadany EF. A summary of demand response in electricity markets. *Electr Power Syst Res* 2008 Nov 1;78(11):1989–96.
- [11] Behrangrad M. A review of demand side management business models in the electricity market. *Renew Sustain Energy Rev* 2015;47:270–83.
- [12] Tan YT, Kirschen D. Classification of control for demand-side participation 29. University of Manchester; 2007.
- [13] Xie D, Hui H, Ding Y, Lin Z. Operating reserve capacity evaluation of aggregated heterogeneous TCLs with price signals. *Appl Energy* 2018;15(216):338–47.
- [14] Hu Q, Li F. Hardware design of smart home energy management system with dynamic price response. *IEEE Trans Smart Grid* 2013;4(4):1878–87.
- [15] Hui H, Ding Y, Liu W, Lin Y, Song Y. Operating reserve evaluation of aggregated air conditioners. *Appl Energy* 2017;15(196):218–28.
- [16] Hui H, Ding Y, Zheng M. Equivalent modeling of inverter air conditioners for providing frequency regulation service. *IEEE Trans Ind Electron* 2019 Feb;66(2):1413–23.
- [17] Shi Q, Li F, Liu G, Shi D, Yi Z, Wang Z. Thermostatic load control for system frequency regulation considering daily demand profile and progressive recovery. *IEEE Trans Smart Grid* 2019.
- [18] Shi Q, Li F, Hu Q, Wang Z. Dynamic demand control for system frequency regulation: concept review, algorithm comparison, and future vision. *Electr Power Syst Res* 2018;1(154):75–87.
- [19] Cai M, Pipattanasomporn M, Rahman S. Day-ahead building-level load forecasts using deep learning vs. traditional time-series techniques. *Appl Energy* 2019;15(236):1078–88.
- [20] Zhang X, Pipattanasomporn M, Rahman S. A self-learning algorithm for coordinated control of rooftop units in small-and medium-sized commercial buildings. *Appl Energy* 2017;1(205):1034–49.
- [21] Siano P, Sarno D. Assessing the benefits of residential demand response in a real time distribution energy market. *Appl Energy* 2016;1(161):533–51.
- [22] Ding Y, Pineda S, Nyeng P, Østergaard J, Larsen EM, Wu Q. Real-time market concept architecture for EcoGrid EU—a prototype for European smart grids. *IEEE Trans Smart Grid* 2013;4(4):2006–16.
- [23] Hui H, Jiang X, Ding Y, Song Y, Guo L. Demonstration of friendly interactive grid under the background of electricity market, reform in China. *IEEE international conference on environment and electrical engineering and 2017 IEEE industrial and commercial power systems Europe (IEEEIC/ICPS Europe)*. 2017. p. 1–5.
- [24] Donnelly M, Trudnowski DJ, Mattix S, Dagle JE. Autonomous demand response for primary frequency regulation. Richland (WA, United States): Pacific Northwest National Lab; 2012.
- [25] Zhang F, Sun Y, Cheng L, Li X, Chow JH, Zhao W. Measurement and modeling of delays in wide-area closed-loop control systems. *IEEE Trans Power Syst* 2015;30(5):2426–33.
- [26] Samarakoon K, Ekanayake J, Jenkins N. Investigation of domestic load control to provide primary frequency response using smart meters. *IEEE Trans Smart Grid* 2012;3(1):282–92.
- [27] Vrettos E, Kara EC, MacDonald J, Andersson G, Callaway DS. Experimental demonstration of frequency regulation by commercial buildings—Part I: Modeling and hierarchical control design. *IEEE Trans Smart Grid* 2018;9(4):3213–23.
- [28] Su L, Norford LK. Demonstration of HVAC chiller control for power grid frequency regulation—Part 2: Discussion of results and considerations for broader deployment. *Sci Technol Built Environ* 2015;21(8):1143–53.
- [29] Beil IB. Fast-timescale control strategies for demand response in power systems; 2015.
- [30] Goddard G, Klose J, Backhaus S. Model development and identification for fast demand response in commercial HVAC systems. *IEEE Trans Smart Grid* 2014;5(4):2084–92.
- [31] Zhao P, Henze GP, Plamp S, Cushing VJ. Evaluation of commercial building HVAC systems as frequency regulation providers. *Energy Build* 2013 Dec;1(67):225–35.
- [32] Lin Y, Barooah P, Meyn S, Middelkoop T. Experimental evaluation of frequency regulation from commercial building HVAC systems. *IEEE Trans Smart Grid* 2015;6(2):776–83.
- [33] Pourmousavi SA, Nehrir MH. Real-time central demand response for primary frequency regulation in microgrids. *IEEE Trans Smart Grid* 2012;3(4):1988–96.
- [34] Pourmousavi SA, Nehrir MH. Introducing dynamic demand response in the LFC model. *IEEE Trans Power Syst* 2014;29(4):1562–72.
- [35] Ayasun S, Nwankpa CO. Impact of demand response on stability region of single-area LFC system with communication delay. *10th International conference on electrical and electronics engineering, 30. IEEE*; 2017. p. 116–9.
- [36] Babahajiani P, Shafiee Q, Bevrani H. Intelligent demand response contribution in frequency control of multi-area power systems. *IEEE Trans Smart Grid* 2018;9(2):1282–91.
- [37] Singh VP, Samuel P, Kishor N. Impact of demand response for frequency regulation in two-area thermal power system. *Int Trans Electr Energy Syst* 2017;27(2):e2246.
- [38] Ledva GS, Vrettos E, Mastellone S, Andersson G, Mathieu JL. Managing communication delays and model error in demand response for frequency regulation. *IEEE Trans Power Syst* 2018;33(2):1299–308.
- [39] Douglass PJ, Garcia-Valle R, Nyeng P, Østergaard J, Tøgeby M. Smart demand for frequency regulation: experimental results. *IEEE Trans Smart Grid* 2013;4(3):1713–20.
- [40] IEEE standard for synchrophasor measurements for power systems. *IEEE Power & Energy Society*; 2011.
- [41] Nanda J, Mishra S, Saikia LC. Maiden application of bacterial foraging-based optimization technique in multiarea automatic generation control. *IEEE Trans Power Syst* 2009;24(2):602–9.
- [42] Information Network of Chinese Business. Analysis on inverter air conditioners in China; 2015. <http://www.askci.com/>.
- [43] Miller R, Chang C. A modified Cramér-Rao bound and its applications (Corresp.). *IEEE Trans Inf Theory* 1978;24(3):398–400.
- [44] Ding Y, Cui W, Zhang S, Hui H, Qiu Y, Song Y. Multi-state operating reserve model of aggregate thermostatically-controlled-loads for power system short-term reliability evaluation. *Appl Energy* 2019.
- [45] Bao Y, Li Y, Wang B, Hu M, Chen P. Demand response for frequency control of multi-area power system. *J Mod Power Syst Clean Energy* 2017;5(1):20–9.
- [46] Razali NM, Wah YB. Power comparisons of Shapiro-Wilk, Kolmogorov-Smirnov, Lilliefors and Anderson-Darling tests. *J Stat Model Anal* 2011;2(1):21–33.